

Repulsive force between screw dislocation and coherent twin boundary in aluminum and copper

Zhiming Chen

Shenyang National Laboratory for Materials Science, Institute of Metal Research, Chinese Academy of Sciences, Shenyang 11006, China

Zhaohui Jin*

School of Materials Science and Engineering, Shanghai Jiao Tong University, Shanghai 200240, China
and Forschungszentrum Karlsruhe, Institut für Nanotechnologie, 76021 Karlsruhe, Germany

Huajian Gao

Division of Engineering, Brown University, Providence, Rhode Island 02912, USA

(Received 28 March 2007; published 21 June 2007)

Molecular dynamics (MD) simulations in combination with an atomistic path technique are used to examine energies required to impinge a screw dislocation on a coherent twin boundary (CTB) in Al and Cu. At large distances, we find that the dislocation-CTB interaction is characterized by repulsive forces which can be attributed to both the elasticity mismatch and distortion (shift and rotation) of deformation fields across the twin boundary. The repulsive forces are determined as a function of distance between the dislocation and the twin boundary based on our MD data and the classical dislocation theory. At short distances, the interaction is significantly influenced by the shear strength of the CTB: relatively low CTB shear strength can induce close-range attractive forces and cause slip to be absorbed into the twin plane.

DOI: 10.1103/PhysRevB.75.212104

PACS number(s): 07.05.Tp, 61.72.Lk, 61.72.Mm

Grain boundaries (GBs) are expected to be effective barriers to hinder dislocation glide in polycrystalline materials.^{1,2} To understand dislocation-GB interactions, one can imagine a straight dislocation, which represents a segment of a curved dislocation or a loop, that is forced to approach an intersecting GB parallel to the dislocation line direction. It is known that the interaction between the dislocation and GB tends to be strongly influenced by the mismatch in elastic properties across the boundary.³⁻⁸ In addition, it has been suggested that the interaction force should also depend on the elastic response of the interface. In this case, the particular structure of a real crystal boundary needs to be considered in order to fully describe the dislocation-GB interaction.⁹⁻¹² For this reason, conventional linear elasticity theory can only provide a partial description of the interaction force as a function of distance between the dislocation and the boundary.

We set out to address the dislocation-GB interaction forces via MD simulations. In particular, we choose to consider a simple but illustrative case: the interaction between a screw dislocation and a coherent twin boundary (CTB),^{13,14} in Al or Cu. The choice is based on recent observations that, besides dislocation-mediated slip, mechanical twinning constitutes an important deformation mode in a number of nanocrystalline (nc) metals including Al.¹⁵⁻¹⁷ On the other hand, strength as well as ductility of nc materials—e.g., nanotwinned Cu—can be limited by dislocation-twin-boundary interactions.¹⁸ To elucidate the physical mechanisms of dislocation reactions at CTBs,^{13,14} the details of which are hardly measurable in *in situ* experiments, it is necessary to examine the elastic energies of a dislocation interacting with a CTB. Such analysis can also be useful for other modeling or simulations of material deformations.^{19,20}

A bicrystal geometry consisting of two twinned grains of nearly equal size separated by a common (111) twin plane (Fig. 1) was used in our simulations. The entire molecular dynamics (MD) cell is measured by $2l_x \sim 85a_0$ in the x di-

rection and $l_y \sim 65a_0$ in the y direction, where a_0 is the lattice parameter equal to 4.05 Å for Al and 3.615 Å for Cu. Periodic boundary conditions were applied in the z direction with a length $l_z = 3\sqrt{2}a_0$. Surface layers perpendicular to the y direction were fixed, and the surface on the right-hand side was set free. The interatomic potentials are based on embedded-atom methods parametrized for Cu and Al.^{21,22} For Cu, a different cutoff scheme has been used for the pair potential functions because the original form leads to non-negligible and unrealistic repulsive forces at the fourth nearest-neighbor distance. A screw dislocation located on the central $(\bar{1}\bar{1}1)$ glide plane was introduced from the left surface of the MD box (for details, see Ref. 13). The Burgers vector is given by $\mathbf{b} = [1\bar{1}0]/2$, and the dislocation line is parallel to the z direction. The perfect dislocation splits into two Shockley

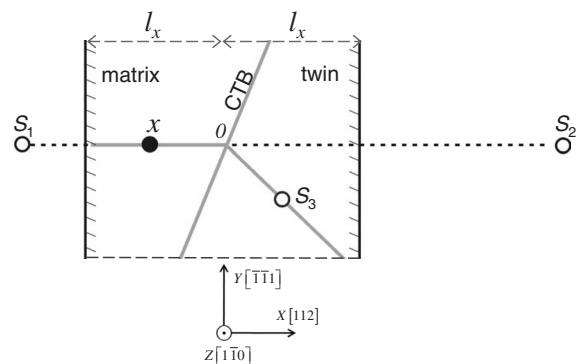


FIG. 1. Schematic plot of a screw dislocation interacting with a CTB in a bicrystal. As the dislocation glides toward the CTB in the x direction, interaction forces arise due to its image dislocations: S_1 and S_2 are the surface images, and S_3 is the twin image. At the CTB ($x=0$), the dislocation may either cross-slip along the CTB or cut through the CTB into the twin grain. Slip pathways (cross-slip and slip transmission) follow the solid lines.

partial dislocations in the glide plane according to $[1\bar{1}0]/2 \rightarrow [2\bar{1}1]/6 + [1\bar{2}\bar{1}]/6$, and the equilibrium splitting width (d_0) between the two partials depends on the elasticity as well as the intrinsic stacking fault energy of the material.^{8,13}

We aimed to monitor the glide motion of the dislocation in the x direction toward the CTB. A driving force is required not only to counterbalance the repulsive force (f_{ctb}) due to the CTB, but also to overcome the image force (f_{surf}) exerted by the two surfaces perpendicular to the moving direction of the dislocation because in this direction our MD box is not infinite. The easiest way to move the dislocation is to apply a simple shear strain (ε) in the y - z shear plane such that the driving force acting on the dislocation is given by the Peach-Koehler force,²³ $\tau = \mu \varepsilon b$, where μ is the $\{111\}\langle 1\bar{1}0 \rangle$ shear modulus equal to 28 GPa for Al and 42 GPa for Cu.

To determine precisely the interaction forces, a combination of MD simulations and the nudged elastic band method (NEB) has been implemented in the present study. The NEB method, rooted from transition-state theory, is an efficient technique for finding the minimum energy path (MEP) between an initial state and a final state of a transition.^{24–26} With this method, the transition path is represented by an elastic band consisting of a set of replicas (intermediate states of a transition) connected by springs. Forces unnecessary to maintain a MEP are to be eliminated through energy minimizations applied simultaneously to the entire band. In our case, replicas are MD configurations corresponding to different stages of dislocation-CTB interactions,¹³ which were recorded in separate MD simulations for a moving dislocation under a constant driving force τ .

Previous studies¹³ have shown that, depending on the driving force and the material, once the screw dislocation impinges on the CTB, the resultant slip may follow two different paths: one is along the common twin plane (cross-slip^{27,28}) and the other is along a glide plane into the neighboring twin grain (slip transmission).^{29–31} Both pathways have been considered in our NEB calculations. For Cu, the MEP can be mapped out for each path, indicating that both pathways are possible to redirect slip at the CTB. For Al, even though the elastic band was set up initially for slip transmission, it ended up with cross-slip; i.e., the dislocation splits into two twinning Shockley partial dislocations along the boundary, indicating that the CTB acts favorably as a sink for the screw dislocation. In these calculations, the elastic bands for slip transmission and cross-slip consist of 16 and 11 replicas, respectively. For each band, the initial and final states were fully relaxed but then fixed during NEB energy minimizations. Furthermore, the climbing-image method²⁵ has been implemented to find the exact minimum energy barrier (the saddle point energy) along a given dislocation reaction path.

The interaction energy (E_i) and position (x) of the dislocation associated with each replica were probed along the MEP after converged NEB calculations. Specifically, E_i is determined according to $(g_i - g_0)/l_z$, where g_0 and g_i are system energies for the initial replica (dislocation positioned at x_0) and the i th replica, respectively, and l_z is the total length of the dislocation in the z direction. As shown in Fig. 2, screw dislocations in either Cu or Al are found to be repelled

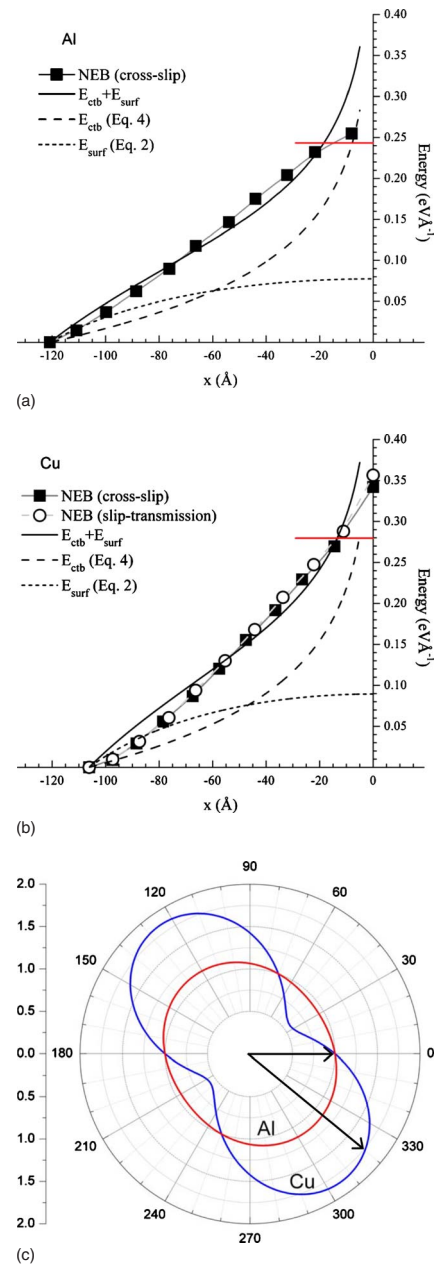


FIG. 2. (Color online) Elastic energies for a screw dislocation interacting with a CTB: NEB data versus theoretical predictions. For Al (a), the data of energy vs position are obtained from the minimum energy pathway (MEP) for cross-slip; for Cu (b), they are obtained from the MEPs for both cross-slip and slip transmission. The maximum NEB energy is the saddle point energy along each pathway. Horizontal lines mark energies at a cutoff distance $\xi = 15$ Å. (c) Rotation about the $\langle 1\bar{1}0 \rangle$ crystal axis changes the shear modulus in the y - z shear plane. The $\{111\}\langle 1\bar{1}0 \rangle$ shear moduli at a zero rotation angle are used to normalize the data. Arrows in the polar plot mark the elasticity mismatch from matrix lattice to twin lattice—i.e., from μ to μ' .

by the CTB; i.e., they tend to move away from the boundary.^{13,14} For Al, the saddle point energy is found to be 0.255 eV/Å at a distance of about 8 Å, beyond which the interaction force becomes attractive. For Cu, the saddle point energies for both pathways are obtained when the dislocation

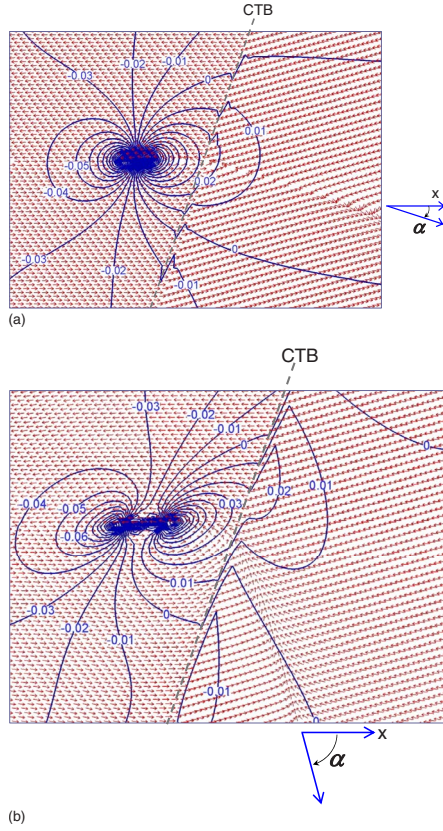


FIG. 3. (Color online) Displacement fields and stress fields about a screw dislocation near a CTB. Atomic displacements are calculated relative to the initial state of the elastic band. For a better view in two dimensions (the x - y plane) and for revealing the direction of flow, the x and z components of the displacement vector have been exchanged and all vectors are plotted at a uniform length. The stress fields are illustrated by isolines of the atomic stress σ_{yz} calculated using the Virial formula (in $\text{eV}/\text{\AA}^3$, $0.01 \text{ eV}/\text{\AA}^3 \approx 1.602 \text{ GPa}$). The dislocations are situated at a position $x \sim -4.5 \text{ nm}$.

reaches the boundary ($x \approx 0$), which yields $0.342 \text{ eV}/\text{\AA}$ for cross-slip and $0.356 \text{ eV}/\text{\AA}$ for slip transmission.

Given that the dislocation motion is purely stress driven, the required shear stress must counterbalance the repulsion—i.e., $\tau = f_{\text{rpl}}$, where the repulsive force ($f_{\text{rpl}} = f_{\text{surf}} + f_{\text{ctb}}$) can be approximated by the slope of the interaction energy if it is treated as a linear function of x . According to $\tau = \mu \epsilon b$, to impinge the dislocation at a position about 1.5 nm away from the CTB, the applied shear strain is close to 0.5% and the corresponding applied shear stress ($\mu \epsilon$) is about 140 MPa for Al and about 220 MPa for Cu, which agree with early simulation results such as for Cu.⁹ The limiting strain or stress can be readily verified via athermal MD simulations.

Image forces due to surfaces (f_{surf}) can be examined by a similar set of simulations but using CTB-free MD geometries. In addition, they can be evaluated in terms of image dislocations according to linear elasticity theory.^{3–6} Two image dislocations are specified for the screw dislocation at x : one at $-2l_x - x$ on the left and the other at $2l_x - x$ on the right (cf. Fig. 1). Under the assumption that the elastic medium is

isotropic with a shear modulus μ , the combination of the stress fields leads to the following force acting on the screw dislocation:

$$f_{\text{surf}} = \frac{\mu b^2}{4\pi} \left(-\frac{1}{l_x + x} + \frac{1}{l_x - x} \right). \quad (1)$$

The work done to move the dislocation from a position x_0 to a new position x ($x_0 < x < 0$) can be obtained by integrating Eq. (1). We have

$$E_{\text{surf}} = \frac{\mu b^2}{4\pi} \left(\ln \frac{l_x + x}{l_x + x_0} - \ln \frac{l_x - x}{l_x - x_0} \right). \quad (2)$$

As shown in Figs. 2(a) and 2(b), the energy E_{surf} contributes nearly 30% of the saddle point energies for Al and Cu. Neglecting the attraction force due to the surface on the right-hand side, nearly 50% of the saddle point energy can be attributed to E_{surf} . Other boundary effects do not change the repulsive forces appreciably.

Our results show that the repulsive forces due to the CTB contribute a major part of the interaction energy when the dislocation is in the vicinity of the boundary. To evaluate the interaction force, a “two-phase” model can be applied if the matrix and twin lattices are treated as materials of different shear moduli.^{3–6} The interaction force between the screw dislocation and the boundary can be represented by introducing a twin-image dislocation (Fig. 1). It follows that

$$f_{\text{ctb}} = -\lambda \frac{\mu b^2}{4\pi x}, \quad (3)$$

and similar to Eq. (2), the interaction energy is given by

$$E_{\text{ctb}} = \lambda \frac{\mu b^2}{4\pi} \ln \frac{x_0}{x}, \quad (4)$$

where the ratio λ is introduced as a dimensionless measure of the interaction strength due to the elasticity mismatch between the matrix and the twin.

Fitting to our NEB data according to $E_i(x) \approx E_{\text{ctb}} + E_{\text{surf}}$, the λ values are estimated to be within a range of 0.5 – 0.8 for both Al and Cu, with and without including the energy contribution due to the free surface on the right-hand side. The repulsion force, or $\lambda > 0$, can be justified in terms of the two-phase model^{3,4} when both the matrix and the twin are treated approximately isotropic. In this case, the ratio is given by $\lambda = 2\mu' / (\mu' + \mu) - 1$, where μ' is the shear modulus of the twin lattice determined by twin-matrix lattice rotation [Fig. 2(c)]. Taking $\mu' \approx 1.85\mu$ for Cu and $\mu' \approx 1.13\mu$ for Al, the corresponding λ ratio is nearly 0.3 for Cu but merely 0.06 for Al, underlying that the simple isotropy treatment, although qualitatively correct, tends to underestimate the repulsive forces.

Anisotropy analyses^{5,6} suggest that the reflection strength (λ) also depends on additional effects, such as the coupling of the displacement and stress fields between the dislocation and its image. As illustrated in Fig. 3, the transmitted stress fields suffer a shift and rotation across the CTB and the slip direction has been potentially deflected from the primary x direction at a clockwise angle ($\alpha \sim 18^\circ$ for Al and $\sim 75^\circ$ for

Cu). The rotation of dislocation-induced stress field across the twin boundary, which is not just limited to the immediate local vicinity of the CTB but also reaches the far field, can exert appreciable influence on the total elastic strain energy. A complete analysis including both anisotropy and nonlinear effects of CTBs lies beyond the scope of our current study.

At large distances, the repulsive forces can be described reasonably well by Eq. (4). As the dislocation approaches the interface, the interaction energy and force become unbounded ($E_{\text{ctb}} \rightarrow \infty$). This arises because the dislocation is treated as an ideal singular dislocation in the continuum theory. Results based on the Peierls model of a screw dislocation^{32,33} show that Eqs. (3) and (4) remain valid for $|x| > 3b$, in agreement with our result that reasonable theoretical predictions can be obtained up to a cutoff distance $\xi \sim 1.5 \pm 0.5$ nm for Al and Cu (Fig. 2).

The strain or stress levels at the dislocation core region can be extremely high. A close examination of our simulation results suggests that dislocation-CTB interactions within cutoff distance ξ are limited by the strength of the CTB against shear. Under ideal circumstance, a CTB in Cu can sustain a shear strain as high as 77% of that for a perfect lattice. For Al, it is reduced to about 50%. This shows that the CTB in Al would yield when the dislocation moves within a distance of about 1 nm, suggesting that the interaction force would become attractive and the dislocation can be spontaneously absorbed into the twin plane.¹³ Such a mechanism also agrees with those proposed previously to understand dislocation interactions with other types of GBs or interfaces.^{9–12}

For Cu, one still needs to consider the recombination of the leading partial and the trailing partial as they are separated at a distance of $d_0 \sim 15$ Å. According to the dislocation theory of linear elasticity, to compress the two partials into a distance ~ 3.5 Å (or $\sim 1.3b$, Ref. 26), the required work is estimated to be 0.04–0.05 eV/Å. Twin symmetry requires

that, for both cross-slip and slip transmission, the redissociation of the fully constricted dislocation at the CTB is equivalent to reversing the order of the two partials associated with the incident dislocation.¹³ Because the activation of dislocation reactions at the CTB is limited by the saddle point energy (E_c), an additional amount of work is required for redissociation, which is about 0.02–0.04 eV/Å. According to Fig. 2, the energy barrier E_c for cross-slip is lower than that for slip transmission by ~ 0.02 eV/Å. Therefore, it is energetically more favorable to redirect the slip along the CTB; however, slip transmissions to the twin grain also occur if the resolved driving force in this direction is larger, which can be further aided by thermal activations and strain rate effects. Our above analyses also offer a link to understanding the dislocation reaction or nucleation in terms of generalized stacking fault energies as suggested in several recent studies.^{13,34,35}

In summary, the interaction force and energy to impinge a screw dislocation upon a CTB have been clarified based on an atomistic path approach. The dislocation-CTB repulsions can be described reasonably well using standard models of dislocations interacting with elastic inhomogeneities. To explain the interaction forces, the coupling between the dislocation and the CTB should be considered. The energy barriers to activate dislocation-CTB reactions are also estimated. Our results provide useful clues to understand fine details of more general and complicated slip transfer involving curved dislocations and multiple dislocations as well as other types of GBs or GB activities.³⁶

The authors gratefully acknowledge P. Gumbsch and K. Lu for valuable discussions. Z.H.J. thanks K.W. Jacobsen for useful suggestions on the NEB methods. This work was supported by NSFC (Grant No. 50621091), MOST of China (Grant No. 2005CB623604), and Deutsche Forschungsgemeinschaft (DFG).

*Author to whom correspondence should be addressed. jinzh@sju.edu.cn

¹A. P. Sutton and R. W. Balluffi, *Interfaces in Crystalline Materials* (Clarendon, Oxford, 1995).

²J. R. Weertman *et al.*, *MRS Bull.* **24**, 44 (1999).

³A. K. Head, *Philos. Mag.* **44**, 92 (1953); A. K. Head, *Proc. Phys. Soc. London, Sect. B* **66**, 793 (1953).

⁴J. Dundurs and G. P. Sendeckyj, *J. Appl. Phys.* **36**, 3353 (1965).

⁵D. M. Barnett and J. Lothe, *J. Phys. F: Met. Phys.* **4**, 1618 (1974).

⁶T. C. T. Ting, *Anisotropic Elasticity: Theory and Applications* (Oxford University Press, New York, 1996).

⁷J. C. M. Li, *Trans. Metall. Soc. AIME* **227**, 239 (1963).

⁸J. P. Hirth and J. Lothe, *Theory of Dislocations* (Wiley, New York, 1982).

⁹S. I. Rao and P. M. Hazzledine, *Philos. Mag. A* **80**, 2011 (2000).

¹⁰M. de Koning *et al.*, *Philos. Mag. A* **82**, 2511 (2002).

¹¹R. G. Hoagland *et al.*, *Scr. Mater.* **50**, 775 (2004).

¹²R. G. Hoagland *et al.*, *Philos. Mag.* **86**, 3537 (2006).

¹³Z. H. Jin *et al.*, *Scr. Mater.* **54**, 1163 (2006).

¹⁴T. Zhu *et al.*, *Proc. Natl. Acad. Sci. U.S.A.* **104**, 3031 (2007).

¹⁵V. Yamakov *et al.*, *Nat. Mater.* **1**, 45 (2002).

¹⁶M. W. Chen *et al.*, *Science* **300**, 1275 (2003).

¹⁷M. A. Meyers *et al.*, *Prog. Mater. Sci.* **51**, 427 (2006).

¹⁸L. Lu *et al.*, *Science* **304**, 422 (2004).

¹⁹V. V. Bulatov *et al.*, *Nature (London)* **440**, 1174 (2006).

²⁰A. Ma *et al.*, *Acta Mater.* **54**, 2181 (2006).

²¹Y. Mishin *et al.*, *Phys. Rev. B* **59**, 3393 (1999).

²²Y. Mishin *et al.*, *Phys. Rev. B* **63**, 224106 (2001).

²³M. Peach and J. S. Koehler, *Phys. Rev.* **80**, 436 (1950).

²⁴H. Jonsson *et al.*, *Classical and Quantum Dynamics in Condensed Phase Systems* (World Scientific, Singapore, 1998).

²⁵G. Henkelman *et al.*, *J. Chem. Phys.* **113**, 9901 (2000).

²⁶T. Rasmussen *et al.*, *Phys. Rev. Lett.* **79**, 3676 (1997).

²⁷B. Escaig, *J. Phys. (Paris)* **29**, 225 (1968).

²⁸W. Püschl, *Prog. Mater. Sci.* **47**, 415 (2002).

²⁹R. L. Fleischer, *Acta Metall.* **7**, 134 (1959).

³⁰S. Mahajan and G. Y. Chin, *Acta Metall.* **21**, 173 (1973).

³¹Z. Shen *et al.*, *Acta Metall.* **36**, 3231 (1988).

³²R. E. Peierls, *Proc. Phys. Soc. London* **52**, 34 (1940).

³³E. S. Pacheco and T. Mura, *J. Mech. Phys. Solids* **17**, 163 (1969).

³⁴Y. Shen and P. M. Anderson, *Acta Mater.* **54**, 3941 (2006).

³⁵M. A. Shehadeh *et al.*, *Philos. Mag.* **87**, 1513 (2007).

³⁶J. W. Cahn *et al.*, *Acta Mater.* **54**, 4953 (2006).